

## Spectroscopic Studies of Charge-Ordering System in Organic Conductors

K. Yakushi,\*<sup>1</sup> K. Yamamoto,<sup>1</sup> R. Świetlik,<sup>1</sup> R. Wojciechowski,<sup>1</sup> K. Suzuki,<sup>1</sup>  
T. Kawamoto,<sup>2</sup> T. Mori,<sup>2</sup> Y. Misaki,<sup>3</sup> K. Tanaka<sup>3</sup>

<sup>1</sup> Institute for Molecular Science, Nishigo-naka, Myodaiji, Okazaki, 444-8585, Japan

<sup>2</sup> Department of Organic and Polymeric Materials, Tokyo Institute of Technology,  
2-12-1, O-okayama, Meguro-ku, Tokyo 152-8552, Japan

<sup>3</sup> Department of Molecular Engineering, Kyoto University, Yoshida-Honmachi,  
Sakyo-ku, Kyoto 606-8501, Japan

**Summary:** Charge localization generates a non-uniform charge distribution in some organic conductors. Phase transitions accompanying such a localization of charge are studied by using infrared and Raman spectroscopy. We first introduce  $\theta$ -(BEDT-TTF)<sub>2</sub>MM'(SCN)<sub>4</sub> (M=Rb, Cs, Tl; M'=Zn, Co) as typical examples of a charge-ordering system, where BEDT-TTF is bis(ethylenedithio)tetrathiafulvalene. We apply the same spectroscopic technique to  $\alpha'$ -(BEDT-TTF)<sub>2</sub>IBr<sub>2</sub>,  $\theta$ -(BDT-TTF)<sub>2</sub>Cu(NCS)<sub>2</sub>, and (TTM-TTP)I<sub>3</sub>, which show the phase transitions from low-resistivity to high-resistivity state, where TTM-TTP is 2,5-bis[4,5-bis(methylsulfonyl)-1,3-dithiol-2-ylidene]-1,3,4,6-tetrathiapentalene.

**Keywords:** charge transfer; infrared spectroscopy; Raman spectroscopy

### Introduction

In molecular conductors, the molecular orbital barely overlaps with those of neighbor molecules. Therefore, the transfer integral ( $t$ ), which contributes to the delocalization of charge, is usually smaller than the on-site ( $U$ ) and off-site ( $V$ ) Coulomb interactions, which contribute to localization of the charges. A strong correlation effect originates from the comparative magnitude of  $t$ ,  $U$ , and  $V$ , and thus many molecular conductors are located at the boundary between a metal (delocalized state) and insulator (localized state). A variety of ground states such as spin-density wave (SDW), charge-density wave (CDW), metal, and superconductivity are found in molecular conductors. For example, the various phases of BEDT-TTF salts are theoretically sorted out with the aid of  $U$ ,  $V$ , and  $t$ .<sup>[1,2]</sup> When the charge is localized, it often induces charge disproportionation (CD) and eventually generates an inhomogeneous charge distribution. This localized state is

called a charge-ordered (CO) state, since the localized charges often form a new periodic structure. Recently, metal-insulator phase transitions accompanying such CO are found in several organic conductors.<sup>[3,4,5,6]</sup> It becomes apparent that the charge ordering is widely associated with metal-insulator phase transitions in a variety of organic conductors. The relationship to unconventional superconductivity is suggested from the viewpoint of experiment<sup>[7]</sup> and theory<sup>[8]</sup>. It is well known that the frequency of some C=C stretching modes of, for example, BEDT-TTF shows a downshift depending upon the degree of oxidation of the molecule.<sup>[9]</sup> Therefore the C=C stretching mode can be used as a probe to detect the charge distribution. Using this principle, we have investigated the CO phase transition. In this paper, we will review the previous study and present the application of the infrared and Raman spectroscopy, which have been conducted in our laboratory.

### $\theta$ -(BEDT-TTF)<sub>2</sub>MM'(SCN)<sub>4</sub> (M=Rb, Co, Tl; M'=Zn, Co)

This system was initiated by Mori *et al.*, and was abbreviated as  $\theta$ -MM'.<sup>[7]</sup>  $\theta$ -RbZn shows a metal-insulator transition at 190 K. Miyagawa *et al.*<sup>[5]</sup> and Chiba *et al.*<sup>[10]</sup> found the existence of CO below the meta-insulator-transition temperature ( $T_{MI}$ ) by <sup>13</sup>C NMR measurements. Mori *et al.*<sup>[7]</sup> and Watanabe *et al.*<sup>[11]</sup> performed the low-temperature x-ray crystal structure analysis, and showed that the unit cell was doubled below  $T_{MI}$  to lower the symmetry. On the other hand,  $\theta$ -CsCo is metal-like down to ~20 K and continuously increases its resistivity below this temperature. In contrast to  $\theta$ -RbZn, the thermopower of  $\theta$ -CsCo exhibits no anomaly at around 20 K. The low-temperature x-ray diffraction experiment shows that a three-dimensional short-range ordering occurs at 20 K, which corresponds with a similar doubling of the unit cell to  $\theta$ -RbZn.<sup>[12]</sup> The low-temperature phase of  $\theta$ -CsCo has not been well characterized.

Figure 1 shows the temperature dependence of the 632.8 nm-excited Raman spectra of  $\theta$ -RbZn and  $\theta$ -CsCo.  $\theta$ -RbZn shows a dramatic change in the spectral region of the C=C stretching region. By contrast,  $\theta$ -CsCo does not show such a drastic change but a continuous change including the growth of the very broad band at around 1250 cm<sup>-1</sup>. The interpretation of  $\theta$ -CsCo has not been made. The lowest-temperature spectrum of  $\theta$ -RbZn was analyzed with the aid of the <sup>13</sup>C-substituted compound as shown in Fig. 2.<sup>[13]</sup> The three C=C stretching modes of BEDT-TTF are classified into IR-active  $\nu_{27}$  ( $b_{1u}$ ) and Raman-active  $\nu_2$  ( $a_g$ ) and  $\nu_3$  ( $a_g$ ).  $\nu_{27}$  is an anti-phase

C=C stretching mode in the five-membered rings, while  $\nu_2$  and  $\nu_3$  are associated with the C=C stretching mode of the central bridge and in-phase mode of the five-membered rings.<sup>[14]</sup> The bridge and ring C=C stretching modes are almost equally mixed in neutral BEDT-TTF<sup>0</sup>. However, they are separated in the (BEDT-TTF)<sub>2</sub><sup>+</sup> dimer,<sup>[15,16]</sup> and  $\nu_2$  and  $\nu_3$  are respectively assigned to the in-phase ring and bridge C=C stretching modes. Therefore  $\nu_3$  is expected to show a large downshift in the <sup>13</sup>C-substituted compound.

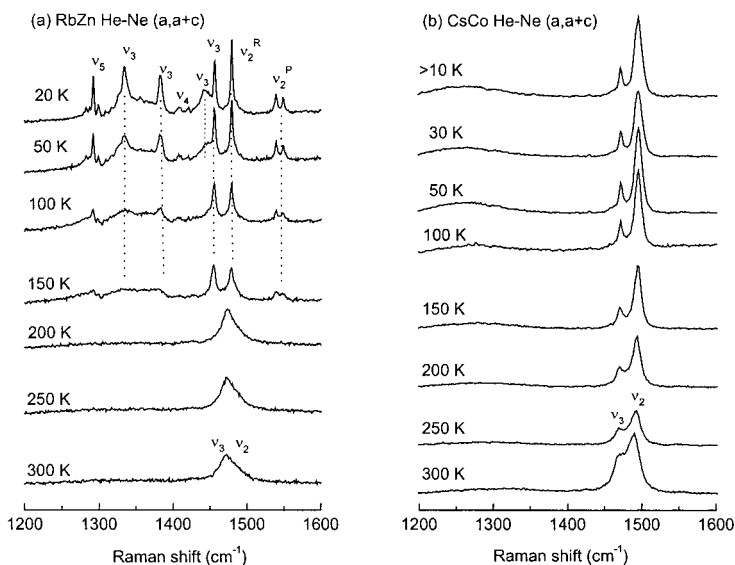


Figure 1. Raman spectra of  $\theta$ -RbZn and  $\theta$ -CsCo excited by a 632.8 nm laser.

Using this property,  $\nu_3$  is separated from  $\nu_2$ ,  $\nu_4$ , and  $\nu_5$  as shown in Fig. 2. Below  $T_{MB}$ , every intramolecular phonon is four-fold degenerate if the intermolecular interaction is very weak, since the unit cell contains four molecules. However,  $\nu_3$  is strongly coupled with the charge-transfer excited state (EMV (electron molecular vibration) coupling).<sup>[17]</sup> Through this EMV interaction, the degenerate  $\nu_3$  is extensively split into four modes. Owing to the EMV interaction, the splitting of  $\nu_3$  does not always signify CD. As discussed in ref. 13, CD is proved by the appearance of  $\nu_3^1(A)$  in the IR E||a spectrum. Another evidence is the splitting of  $\nu_2$  in the same polarization [See (a,a) polarization]. Since  $\nu_2$  has a weak EMV interaction, the splitting of  $\nu_2$  originates almost purely from the difference in oxidation degree, so that the deviation from +0.5 in (BEDT-

$\text{TTF}^{0.5+\delta}(\text{BEDT-TTF})^{0.5-\delta}$  is estimated as  $\delta=0.35$  from the separation between  $\nu_2^{\text{P}}$  (charge-poor site) and  $\nu_2^{\text{R}}$  (charge-rich site).

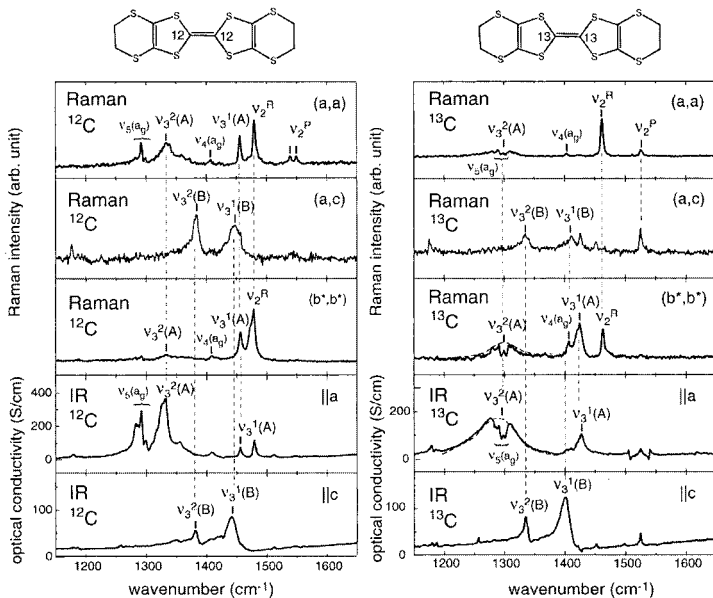


Figure 2. Polarized Raman spectra of natural and  $^{13}\text{C}$ -substituted  $\theta$ -RbZn. For example, (a,c) show that the laser and scattered light are polarized along the a- and c-axes, respectively, in the back scattering geometry.

Another important information from Fig. 2 is the selection rule that the A and B symmetry modes are separately observed in different polarizations. This selection rule proves that the glide-plane symmetry is preserved at this temperature. Therefore, the charge-rich sites connected by the glide-plane symmetry are aligned along the a-axis to form a horizontal stripe. The conclusion is that  $\nu_2$  can be used to estimate the CD ratio and  $\nu_3$  can be used to examine the symmetry. The interpretation of the spectrum above  $T_{\text{MI}}$  is more difficult, since the spectrum shows a single broad band with a non-Lorentzian lineshape.  $\nu_2$  and  $\nu_3$  are well separated and observed, respectively, at  $1474\text{ cm}^{-1}$  and  $1503\text{ cm}^{-1}$  in a metallic BEDT-TTF compound,  $\kappa$ -(BEDT-TTF) $_2\text{Cu}[\text{N}(\text{CN})_2]\text{Br}$ .<sup>[16]</sup> They are not completely separated in the room-temperature spectrum of  $\theta$ -CsCo, which is more metallic than  $\theta$ -RbZn. The spectral shape seems to be associated with the fluctuation of charge density. In the case of  $\theta$ -RbZn, we speculate that the charge is nearly

localized above  $T_{MI}$  and is extensively fluctuating around  $\delta=0$  owing to the incoherent hopping. We have investigated the  $\theta$ -TiZn and  $\theta$ -TiCo using the same method. In this process, we found an orthorhombic phase of  $\theta$ -TiZn in addition to a monoclinic phase of  $\theta$ -TiZn. Since the orthorhombic phases of  $\theta$ -TiZn and  $\theta$ -TiCo are isostructural to  $\theta$ -RbZn, the spectral change at the phase transition temperature is almost exactly the same as that of  $\theta$ -RbZn except for the transition temperature. However, the spectral change of monoclinic  $\theta$ -TiZn gradually occurs at much higher temperature ( $\sim 250$  K) than  $T_{MI}$  ( $\sim 165$  K). Probably the charge is more fluctuating than in  $\theta$ -RbZn above  $T_{MI}$ .

### $\alpha'$ -(BEDT-TTF)<sub>2</sub>IBr<sub>2</sub>

This compound is non-metallic and shows a phase transition at 200 K from low- to high-resistivity state.<sup>[18]</sup> Although the structural change is investigated by x-ray diffraction, no drastic change has been detected at 200 K.<sup>[19,20]</sup> Since the band calculation suggests a semimetallic

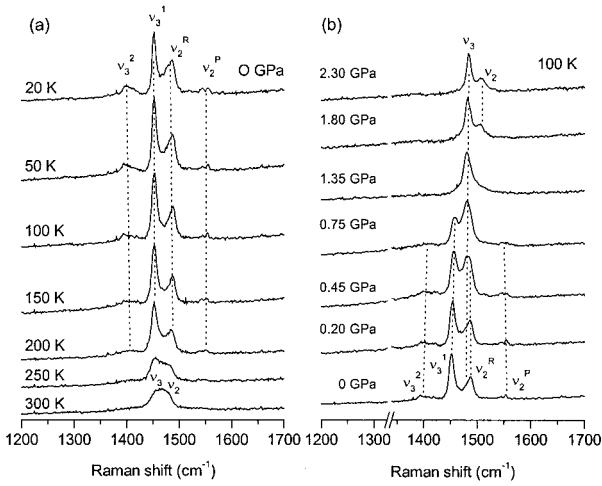


Figure 3. Temperature and pressure dependence of the Raman spectrum of  $\alpha'$ -(BEDT-TTF)<sub>2</sub>IBr<sub>2</sub>.

band, one of the scenarios for this phase transition is the gap enhancement caused by a small structural change in a narrow-gap semiconductor. However, the spin degrees of freedom are preserved below 200 K. Thus the localization of charge is more plausible for the mechanism of the phase transition at 200 K.

Based on the knowledge of the assignment in  $\theta$ -RbZn, we applied Raman spectroscopy to this phase transition. Figure 3a shows the temperature dependence of the Raman spectra excited by a 514.5 nm laser. The broad room-temperature spectrum resembles that of  $\theta$ -RbZn shown in Fig. 1a. At 200 K, the spectrum shows a clear splitting, and the broad band splitting into four or six at 20 K. Based on the assignment shown in Fig. 1a, the disproportionation ratio is estimated as  $\delta \sim 0.4$ . The molecules are stacked along the  $a$ -axis, and the unit cell contains two independent stacks. In each stack, two molecules are connected by inversion symmetry. Therefore the unit cell contains four molecules. If the center of symmetry is preserved, each mode is classified into two in-phase ( $A_g$ ) and two out-of-phase ( $A_u$ ) modes, and only the  $A_g$  mode is Raman-active. There are two modes  $\nu_2$  and  $\nu_3$  in this spectral region, so that four bands should be observed at most if the center of symmetry is preserved at 20 K. Figure 3a suggests the conservation of the center of symmetry below  $T_M$ . Figure 3b shows the pressure dependence of the spectrum at 100 K. On increasing pressure, the four bands continuously decrease in intensity, and disappear at 1.35 GPa. Instead, a new band at  $\sim 1475 \text{ cm}^{-1}$  grows up, and finally the spectrum shows well-resolved  $\nu_2$  and  $\nu_3$ , which are similar to those of a metallic BEDT-TTF salt. We speculate that the charge distribution is homogeneous at 2.3 GPa. High pressure appears to be more effective in increasing  $t$  than  $U$  and  $V$ .

### $\theta$ -(BEDT-TTP)<sub>2</sub>Cu(NCS)<sub>2</sub>

The CO phase transition was found by Ouyang *et al.* in this compound, which was synthesized by Misaki *et al.*<sup>[21]</sup> The weakly dimerized  $\beta$ -type of BDT-TTP salts such as (BDT-TTP)<sub>2</sub>SbF<sub>6</sub> is metallic down to 2 K and shows a typical Drude-type reflectivity down to  $600 \text{ cm}^{-1}$ .<sup>[22,23]</sup> However, the  $\theta$ -type salt,  $\theta$ -(BDT-TTP)<sub>2</sub>Cu(NCS)<sub>2</sub>, is non-metallic up to 350 K as shown in Fig. 4a. The structure resembles that of monoclinic  $\theta$ -(BEDT-TTF)<sub>2</sub>TiZn(SCN)<sub>4</sub>.<sup>[24]</sup> This compound shows a sharp increase in resistivity at  $\sim 250 \text{ K}$ . The optical conductivity obtained from the Kramers-Kronig transformation of the reflectivity spectrum also shows a remarkable change at  $\sim 250 \text{ K}$ . The spectral weight less than  $2000 \text{ cm}^{-1}$  shifts to the high-wavenumber region, and thus the optical gap continuously increases near the phase transition temperature. The localization and disproportionation of the charge below the phase transition temperature is proved by the Raman spectrum.

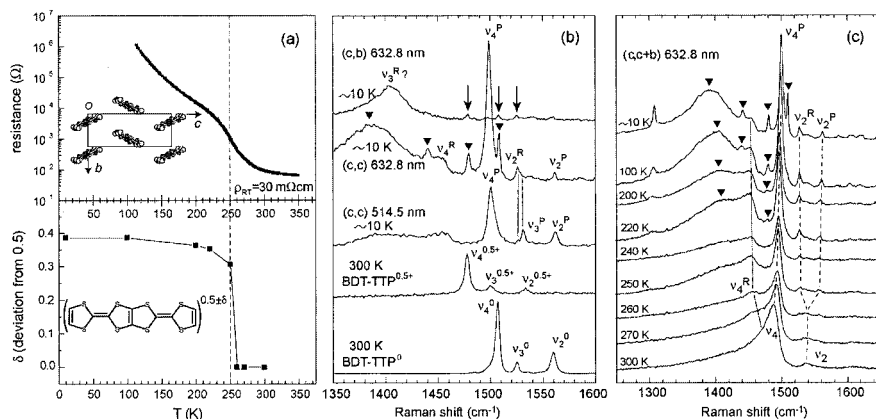


Figure 4. (a) Electric resistance and disproportionation ratio  $\delta$ , (b) comparison of the Raman spectra, and (c) temperature dependence of the Raman spectrum of  $\theta$ -(BDT-TTP)<sub>2</sub>Cu(NCS)<sub>2</sub>.

Before explaining the Raman spectra in Figs. 4b and 4c, let us introduce the normal coordinate analysis reported by Ouyang *et al.*<sup>[25]</sup> The five C=C stretching modes are named as Raman-active  $v_2, v_3$ , and  $v_4$  and infrared-active  $v_{21}$  and  $v_{22}$ . These modes are rather isolated from other fundamental modes. The five C=C stretching modes are significantly mixed in BDT-TTP<sup>0</sup>, whereas they are rather separated in BDT-TTP<sup>+</sup>. Thus  $v_2$  and  $v_3$  in BDT-TTP<sup>+</sup> are assigned mainly to the in-phase mode of the C=C stretching of outer rings and bridges,  $v_4$  is assigned to the C=C stretching of the inner ring,  $v_{21}$  and  $v_{22}$  are assigned to the out-of-phase modes of the C=C stretching of outer rings and bridges, respectively. As shown in Fig. 4b, the three Raman-active modes show a low-frequency shift by 20–25 cm<sup>-1</sup> from BDT-TTP<sup>0</sup> to BDT-TTP<sup>0.5+</sup>. These modes can become a good probe to detect the oxidation state. As shown in Fig. 4c, the Raman spectrum in the C=C stretching regions dramatically changes below the phase transition temperature. In Fig. 4b, the Raman spectra excited by 632.8 nm are compared with those excited by 514.5 nm. Since 514.5 nm is close to the first excited state of BDT-TTP<sup>0</sup>, the Raman modes associated with BDT-TTP<sup>0</sup> are enhanced owing to the resonance effect. If we take the resonance effect into account, the resemblance of (c,c) spectrum excited by 514.5 nm to that of BDT-TTP<sup>0</sup> straightforwardly leads to the view that the charge disproportionation occurs at  $\sim 10$  K. Based on the temperature dependence shown in Fig. 4c, we assigned the Raman bands at  $\sim 10$  K as shown

in Fig. 4b. Although the  $\sim 10$  K spectrum is complicated, the spectrum near the phase transition, for example 240 K, is easily interpreted. At this temperature, both  $\nu_2$  and  $\nu_4$  are split into the modes corresponding to the charge-poor ( $\nu_j^P$ ) and charge-rich ( $\nu_j^R$ ) sites. From the separation between  $\nu_2^P$  and  $\nu_2^R$ , the disproportionation ratio  $\delta$  is estimated as shown in the bottom panel of Fig. 4a. This parameter is regarded as the order parameter of this phase transition.

Additional bands marked by triangles appear below 220 K as shown in Fig. 4c. The appearance of these additional bands signifies the doubling of the unit cell including the short-range order. As indicated by arrows in Fig. 4b, three bands appear in (c,c) as well as in (c,b) polarization. The appearance of these bands indicates that the glide-plane symmetry is broken at  $\sim 10$  K. We have examined this selection rule at 200 K, and have found the breaking of the selection rule. Therefore, we speculate that the localized charge is aligned along the b-axis.

### (TTM-TTP)I<sub>3</sub>

The high conductivity ( $\sigma_{RT} \sim 10^3$  S/cm) of (TTM-TTP)I<sub>3</sub> attracted attention, because this compound is a half-filled quasi-one-dimensional system. The electric resistivity is almost temperature-independent down to  $\sim 160$  K and steeply increases below this temperature.<sup>[26]</sup> Below  $\sim 160$  K, the lattice is doubled ( $2k_F$  modulation) and the electronic system undergoes a spin singlet state.<sup>[27,28]</sup> Onuki *et al.* proposed through the solid-state NMR experiment that a charge disproportionation such as  $(\text{TTM-TTP})^{(1+\delta)+}$   $(\text{TTM-TTP})^{(1-\delta)+}$  accompanied this phase transition.<sup>[29]</sup> We applied the vibrational spectroscopy to this phase transition if such inhomogeneous charge distribution appeared. Since this molecule has the same  $\pi$ -conjugated skeleton as BDT-TTP, we use the same notation for the C=C stretching modes as BDT-TTP for convenience.

TTM-TTP is stacked along the c-axis. A strong  $\nu_{22}$  mode was observed in the  $E \perp c$  reflection spectrum. In the low-temperature optical conductivity,  $\nu_{22}$  showed neither shift nor splitting down to 20 K. Since the frequency of  $\nu_{22}$  is most sensitive to the charge among the five C=C stretching modes, this observation clearly indicates that the charge disproportionation does not occur at the phase transition temperature,  $\sim 160$  K. At room temperature, the Raman-active modes were observed at  $\nu_2 = 1490$  cm<sup>-1</sup>,  $\nu_3 = 1455$  cm<sup>-1</sup>, and  $\nu_4 = 1433$  cm<sup>-1</sup>, when 514.5 nm laser was used. Figure 5a shows the Raman spectra measured by 785 nm excitation, in which  $\nu_4$  is missing in



(TTM-TTP) $I_3$ . As shown in this figure,  $\nu_3$  shows no change below  $\sim 160$  K, whereas  $\nu_2$  splits into two bands at  $1487\text{ cm}^{-1}$  and  $1499\text{ cm}^{-1}$  at  $155$  K. Since the charge disproportionation is not found in  $\nu_{22}$ , we interpret that this splitting is caused by the asymmetric deformation of the molecule. In other words, the center of symmetry of the molecule is broken below  $\sim 160$  K due to the structural change ( $2k_F$  modulation). When the molecule has a center of symmetry, the C=C stretching modes of the outer five-membered rings are classified into the Raman-active in-phase mode  $\nu_2$  and infrared-active out-of-phase mode  $\nu_{21}$ . The frequencies of  $\nu_2$  and  $\nu_{21}$  are close, because these two C=C bonds are far from each other.<sup>[25]</sup> If the symmetry is broken and two C=C bonds become non-equivalent, these two modes mix with each other and both modes become infrared and Raman active.

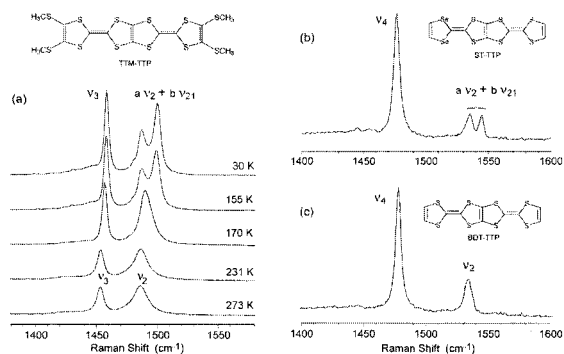


Figure 5. Raman spectra of (TTM-TTP) $I_3$ , (ST-TTP) $_2\text{AsF}_6$ , and (BDT-TTP) $_2\text{SbF}_6$ .

To confirm this speculation, we measured the Raman spectra of the isostructural charge-transfer salts of symmetric BDT-TTP and asymmetric ST-TTP. When we use 785 nm laser,  $\nu_3$  is missing in both compounds. As shown in Fig. 5a and 5b,  $\nu_2$  shows no splitting in (BDT-TTP) $_2\text{SbF}_6$ , whereas  $\nu_2$  shows a clear splitting with the separation  $10\text{ cm}^{-1}$  in (ST-TTP) $_2\text{AsF}_6$ . This separation is very close to that ( $12\text{ cm}^{-1}$ ) of (TTM-TTP) $I_3$  below  $\sim 160$  K. This observation strongly supports our speculation. Usually the asymmetric environment around the molecule does not have such a big influence on the molecular structure, since the stabilization energy by  $\pi$ -conjugation is much larger than the intermolecular interaction. This long molecule structure may have an inherent instability to the asymmetric distortion.<sup>[30-32]</sup>

- [1] H. Kino, H. Fukuyama, *J. Phys. Soc. Jpn.* **1996**, 65, 2158.
- [2] H. Seo, *J. Phys. Soc. Jpn.* **2000**, 69, 805.
- [3] K. Hiraki and K. Kanoda, *Phys. Rev. Lett.* **1998**, 80, 4737.
- [4] D. S. Chow, F. Zamborsky, A. Alavi, D. J. Tantillo, A. Bauer, C. A. Merlic, and S.E. Brown, *Phys. Rev. Lett.* **2000**, 85, 1698.
- [5] K. Miyagawa, A. Kawamoto, K. Kanoda, *Phys. Rev. B* **2000**, 62, R7679.
- [6] J. Ouyang, K. Yakushi, Y. Misaki, and K. Tanaka, *Phys. Rev. B* **2001**, 63, 054301.
- [7] H. Mori, S. Tanaka, T. Mori, *Phys. Rev. B* **1998**, 57, 12023.
- [8] J. Merino and R. H. McKenzie, *Phys. Rev. Lett.* **2001**, 87, 237002.
- [9] M. E. Kozlov, K. I. Pokhodnia, A. A. Yurchenko, *Spectrochim. Acta* **1989**, 45A, 437.
- [10] R. Chiba, H. M. Yamamoto, K. Hiraki, T. Nakamura, T. Takahashi, *Synth. Met.* **2001**, 120, 919.
- [11] M. Watanabe, Y. Noda, Y. Nogami, H. Mori, private communication.
- [12] M. Watanabe, Y. Nogami, K. Oshima, H. Mori, S. Tanaka, *J. Phys. Soc. Jpn.* **1999**, 68, 2654.
- [13] K. Yamamoto, K. Yakushi, K. Miyagawa, and K. Kanoda, and A. Kawamoto, *Phys. Rev. B* **65**, 085110 (2002).
- [14] M. E. Kozlov, K. I. Pokhodnia, A. A. Yurchenko, *Spectrochim. Acta* **1987**, 43A, 323.
- [15] J. E. Eldridge, Y. Xie, H. H. Wang, J. M. Williams, A. M. Kini, J. A. Schlueter, *Mol. Cryst. Liq. Cryst.* **1996**, 284, 97.
- [16] M. Maksimuk, K. Yakushi, H. Taniguchi, K. Kanoda, A. Kawamoto, *J. Phys. Soc. Jpn.* **2001**, 70, 3728.
- [17] J. E. Eldridge, K. Kornelsen, H. H. Wang, J. M. Williams, A. V. Strieby Crouch, D. M. Watkins, *Solid State Commun.* **1991**, 79, 583.
- [18] M. Tokumoto, H. Anzai, T. Ishiguro, *Synth. Met.* **1987**, 19, 215.
- [19] Y. Nogami, S. Kagoshima, T. Sugano, G. Saito, *Synth. Met.* **1986**, 16, 367.
- [20] M. Watanabe, M. Nishikawa, Y. Nogami, K. Oshima, G. Saito, *J. Korean Phys. Soc.* **1997**, 31, 95.
- [21] J. Ouyang, K. Yakushi, Y. Misaki, and K. Tanaka, *Phys. Rev. B* **2001**, 63, 054301.
- [22] T. Nakada, T. Ishiguro, T. Miura, Y. Misaki, T. Yamabe, T. Mori, *J. Phys. Soc. Jpn.* **1998**, 67, 355.
- [23] J. Ouyang, K. Yakushi, Y. Misaki, K. Tanaka, *J. Phys. Soc. Jpn.* **1998**, 67, 3191.
- [24] H. Mori, S. Tanaka, T. Mori, A. Kobayashi, and H. Kobayashi, *Bull. Chem. Soc. Jpn.* **1998**, 71, 797.
- [25] J. Ouyang, K. Yakushi, T. Kinoshita, N. Nanbu, M. Aoyagi, Y. Misaki, and K. Tanaka, *Spectrochim. Acta Part A* **2002**, 58, 1643.
- [26] T. Mori, T. Kawamoto, J. Yamaura, T. Enoki, Y. Misaki, T. Yamabe, H. Mori, and S. Tanaka, *Phys. Rev. Lett.* **1997**, 79, 1702.
- [27] M. Maesato, Y. Sasou, S. Kagoshima, T. Mori, T. Kawamoto, Y. Misaki, T. Yamabe, *Synth. Met.* **1999**, 103, 2109.
- [28] N. Fujimura, A. Namba, T. Kambe, Y. Nogami, K. Oshima, T. Mori, T. Kawamoto, Y. Misaki, T. Yamabe, *Synth. Met.* **1999**, 103, 2111.
- [29] M. Onuki, K. Hiraki, T. Takahashi, D. Jinno, T. Kawamoto, T. Mori, K. Tanaka, and Y. Misaki, *J. Phys. Chem. Solids* **2001**, 62, 405.
- [30] S. F. Rak and L. L. Miller, *J. Am. Chem. Soc.* **1992**, 114, 1388.
- [31] K. Lahil, A. Moradpour, C. Bowlas, F. Menou, P. Cassoux, J. Bonvoisin, J.-P. Launay, G. Dive, and D. Dehareng, *J. Am. Chem. Soc.* **1995**, 117, 9995.
- [32] K. Pokhodnia, P. Cassoux, J. Bonvoisin, a. Mlayah, L. Brossard, S. Frenzel, oand K. Mullen, *J. Phys. Chem. B* **1997**, 101, 3665.